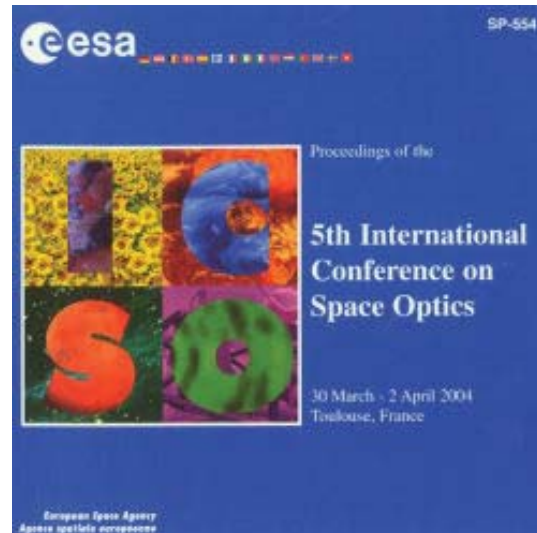


International Conference on Space Optics—ICSO 2004

Toulouse, France

30 March–2 April 2004

Edited by Josiane Costeraste and Errico Armandillo



Grism and immersion grating for space telescope

Noboru Ebizuka, Kiko Oka, Akiko Yamada, Mami Ishikawa, et al.



GRISM AND IMMERSION GRATING FOR SPACE TELESCOPE

Noboru Ebizuka^(1,6), Kiko Oka^(1,2), Akiko Yamada⁽²⁾, Mami Ishikawa⁽²⁾, Masako Kashiwagi⁽²⁾, Kashiko Kodate⁽²⁾, Yasuhiro Hirahara⁽³⁾, Shuji Sato⁽³⁾, Koji S. Kawabata⁽⁴⁾, Moriaki Wakaki⁽⁵⁾, Shinya Morita⁽¹⁾, Tomoyuki Simizu⁽¹⁾, Shaohui Yin⁽¹⁾, Hithoshi Omori⁽¹⁾ and Masanori Iye⁽⁶⁾

⁽¹⁾ Integrated V-CAD System Research Program, RIKEN (The Institute of Physical and Chemical Research), Wako, Saitama 351-0198 Japan, e-mail: ebizuka@riken.go.jp

⁽²⁾ Faculty of Sciences, Japan Women's University

⁽³⁾ Faculty of Sciences, Nagoya University

⁽⁴⁾ Faculty of Sciences, Hiroshima University

⁽⁵⁾ Faculty of engineering, Tokai University

⁽⁶⁾ National Astronomical Observatory of Japan

ABSTRACT

The grism is a versatile dispersion element for an astronomical instrument ranging from ultraviolet to infrared. Major benefit of using a grism in a space application, instead of a reflection grating, is the size reduction of optical system because collimator and following optical elements could locate near by the grism. The surface relief (SR) grism is consisted a transmission grating and a prism, vertex angle of which is adjusted to redirect the diffracted beam straight along the direct vision direction at a specific order and wavelength. The volume phase holographic (VPH) grism consists a thick VPH grating sandwiched between two prisms, as specific order and wavelength is aligned the direct vision direction. The VPH grating inheres ideal diffraction efficiency on a higher dispersion application. On the other hand, the SR grating could achieve high diffraction efficiency on a lower dispersion application. Five grisms among eleven for the Faint Object Camera And Spectrograph (FOCAS) of the 8.2m Subaru Telescope with the resolving power from 250 to 3,000 are SR grisms fabricated by a replication method. Six additional grisms of FOCAS with the resolving power from 3,000 to 7,000 are VPH grisms. We propose "Quasi-Bragg grism" for a high dispersion spectroscopy with wide wavelength range.

The germanium immersion grating for instance could reduce 1/64 as the total volume of a spectrograph with a conventional reflection grating since refractive index of germanium is over 4.0 from 1.6 to 20 μm . The prototype immersion gratings for the mid-InfraRed High dispersion Spectrograph (IRHS) are successfully fabricated by a nano-precision machine and grinding cup of cast iron with electrolytic dressing method.

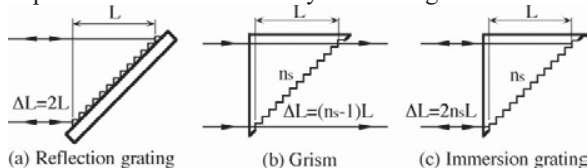


Fig. 1. Gratings

1. Introduction

The direct vision grating, namely, the grism (Fig.1b) is a versatile dispersion element for an astronomical observations ranging from ultraviolet to infrared. Major benefit of using a grism in a space application, instead of a reflection grating (Fig.1a), is the size reduction of optical system because collimator and following optical elements could locate near by the grism (Fig.2). Moreover, the grism has the possibility for allowing flexible switching between imaging and spectroscopic mode by simply inserting or removing the grism in the optical pass.

The immersion grating (Fig.1c) is filled up a dielectric medium in its optical pass and the angular dispersion of the grating is proportional to the refractive index of the medium. The total volume of a spectrograph could dramatically reduce by means of an immersion grating since the volume of the spectrograph is inversely proportional to the cubic of the refractive index of the grating media.

We introduce function of grism and immersion grating and the fabrication methods on gratings developed for instruments of the 8.2m Subaru Telescope on Mauna Kea, Hawaii [1-3].

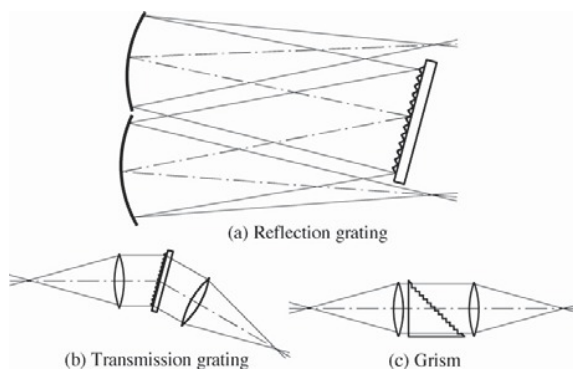


Fig. 2 Size comparison of grating spectrographs.

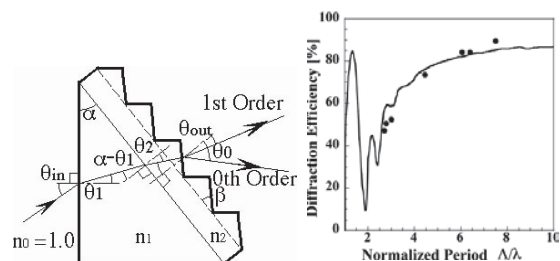


Fig. 3 Schematic representation (left) and diffraction efficiency (right) of surface relief grism.

2. Grism

2.1. Surface relief grism

As shown in figure 3 left, a surface relief (SR) grism is consisted a transmission grating and prism, vertex angle of which is adjusted to redirect the diffraction beam straight along the direct vision direction at a specific order and wavelength. This type of grism has been used for astronomical instruments until multi-channel detectors such as a CCD had developed. Especially, a replica of a blazed grating is generally used for a low dispersion grism of visible and near infrared instruments because it is moderate prices and sufficient diffraction efficiency for general purpose [4]. However, as groove period of a SR grating is close to functional wavelength, diffraction efficiency behaves peculiarly. The cause of the phenomena is an electromagnetic coupling of higher order diffraction and periodic grating structure, namely, anomaly. Figure 3 right shows calculated and measured diffraction efficiency versus normalized period of a SR transmission grating with refractive index of 1.5. The calculations are carried out by means of the analysis program valid for gratings of the rigorous coupled-wave analysis (RCWA) method [5]. The efficiency of the SR grating become oscillatory decrease below 5 and steeply drops at 2 in normalized groove period. Measured efficiencies of SR grisms (closed dots) are compatible with the efficiency cave of the RCWA calculation.

The grism with higher order diffractions, that is, Echelle type grism are used for the high dispersion spectrograph on astronomical observations. High index material is employed for the prism of a high dispersion grism if the grism size is limited by space of an instrument since dispersion is proportional to optical path difference caused by the grating (Fig. 1). However when a grism consists of a high index prism and replicated grating, the vertex angle of the prism is limited by a critical angle between the high index material and resin of replica. Refractive indices of the prism and replica of a SR grism are 2.3 and 1.5 respectively for example, and a ray enters vertically from the prism side, the critical angle is 40.7 degree, that is, a vertex angle of the prism has to be smaller

than the critical angle. In the case of the grism tilts to clockwise in figure 3 left, critical angle becomes larger, and optical axes are sifted in parallel between the incident and exit ray on the grism. The following optics of an instrument becomes lager to avoid the vignetting at a result of the optical axes shift. In these reason, a SR grism with high dispersion is essentially grooved directly onto a high index material that is called a solid grating.

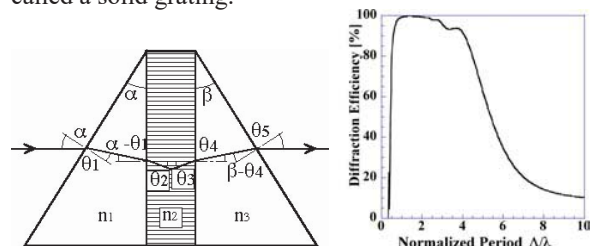


Fig. 4 Schematic representation (left) and diffraction efficiency (right) of volume phase holographic grism.

2.2. Volume phase holographic grism

The volume phase holographic (VPH) grism consists a thick VPH grating sandwiched between two prisms as specific order and wavelength is aligned the direct vision direction (Fig. 4 left). As show in figure 4 right, a thick VPH grating archives very high efficiency from 1 to 5 in normalized period of index modulation [5]. In the case of the VPH grism, refractive indices of prisms and VPH grating are 2.3 and 1.5 respectively α is obtained 63.6 degree from Eq.4 in Appendix A. As mentioned in subsection 2.1, the vertex angle of the prism is limited by the critical angle between a grating replica and prism. It means that a VPH grism has capability of higher dispersion spectroscopic observations compared with a SR grism. However a thick volume phase grating was very difficult to fabrication owing to recoding media. Dichromate gelatin had been the unique recording media for a thick volume phase hologram in practical use [6], preparation of recording material and development are complicated and critical because they are wet process.

We applied a photosensitive resin developed by Nippon Paint Co.Ltd. as a recording material of VPH grating. The photosensitive resin could overcome the disadvantages of dichromate gelatin [7-8]. The photosensitive resin consists of radically polymerizable monomer (RPM) with higher refractive, cationically polymerizable monomer (CPM) with lower refractive index, dyes, and photo-initiator. By accepting the radical from dyes absorbed visible light (470-600nm), the RMP is polymerized (Fig.7). Consequently, the monomer of RMP produces the concentration gradients at the boundary between the polymerized part and the unpolymerized part. Because of monomer diffusion, the refractive index of the polymerized part becomes higher. RPM and CPM are simultaneously

polymerized by the photo-initiator with ultraviolet irradiation, and the refractive index modulation is fixed.

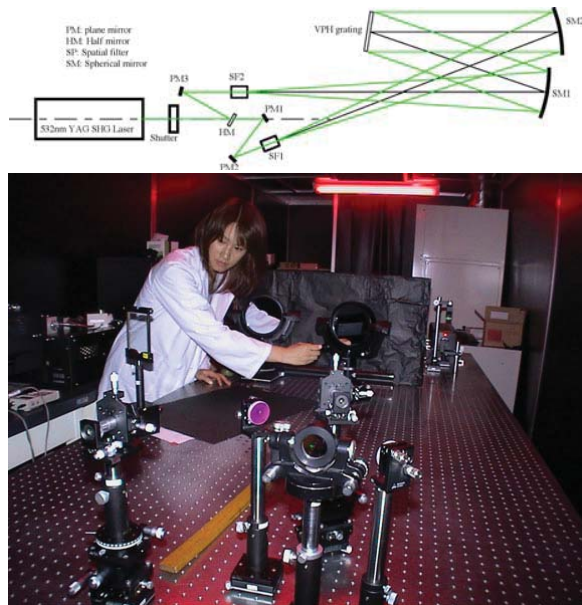


Fig. 5 Schematic representation (above) and picture (below) of optical system for VPH grating exposure.

2.3. Grisms for Subaru Telescope

Several types of diffraction grating are developed for instruments of the 8.2m Subaru Telescope on Mauna Kea, Hawaii [9-11]. Trispec grisms for visible, J-H band and K band were made by replication. The solid grism of Cytop (fluorocarbon polymers) for the Coronagraphic Imager with Adaptive Optics (CIAO) with the resolving power of 600 at near infrared had been successfully fabricated by using a 3D profiling machine with nano-precision and diamond turning method. The Cytop is transparent from 200 to 2,500 nm. Moreover, a solid grism of gallium arsenide (GaAs) or ZnSe with higher dispersion for CIAO ranging from 0.9 to 5 μm are under developing. The Faint Object Camera And Spectrograph (FOCAS) is providing eleven grisms with the resolving power from 250 to 7,000 [12-16].

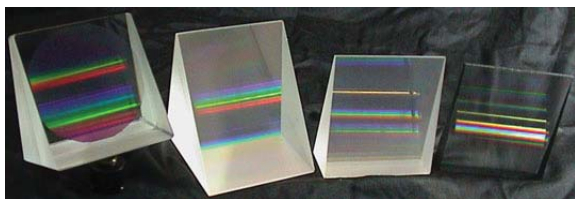


Fig. 6 FOCAS grisms. From right, replicated grisms with low dispersion ($R=500$ with 0.4" slit), middle dispersion ($R=1,400$) and Echelle type (higher order diffraction) with high dispersion ($R=3,000$), VPH grism with high dispersion ($R=3,000$)

2.4. FOCAS grisms

The physical size of a FOCAS grism is 110 by 106 mm, the maximum thickness along the optical axis is 106 mm. Five FOCAS grisms among eleven were made by replication onto a prism of conventional optical glass (Fig.6 right to center left) and residual six are VPH grisms (Fig.6 left). Grisms of high dispersion with the first diffraction order were fabricated by replication. However, measured efficiencies of the grisms are 45 to 48 % at the each blazed wavelength as the result of anomaly (Fig. 3 left, Normalized period: 2.70 and 2.78). The value could not be sufficient for the specifications of FOCAS.

We employed VPH grisms (Fig. 4 left) for the high ($R=3,000$) and very high ($R=7,000$) dispersion grisms of FOCAS with the first diffraction order because a VPH grating is suitable for a higher dispersion application as shown in figure 4 right [5]. The VPH grism with high dispersion consist of a VPH grating two prisms of a conventional optical glass (Fig. 6 left). The very high dispersion grisms with the first order diffraction consist of a VPH grating and two high-index prisms of zinc selenide (ZnSe , $n=2.6$) as shown in figure 7.



Fig. 7 ZnSe VPH grism for FOCAS with very high dispersion ($R=7,000$).

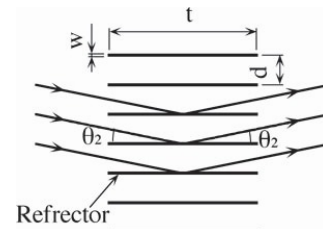


Fig. 8 Schematic representation of "Quasi-Bragg grating".

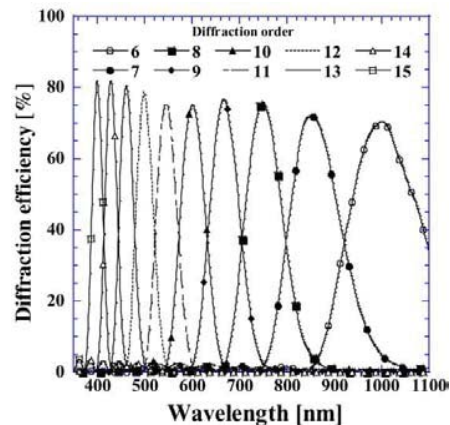


Fig.9 Calculation result of diffraction efficiencies of Quasi-Bragg grating [18]. (Al refractor, $d=15.27 \mu\text{m}$, $\Lambda=5.71 \mu\text{m}$, $w=0.029 \mu\text{m}$, $n_g=1.50$, Bragg angle : $\theta_B=20.51\text{deg}$)

2.5. Quasi-Bragg grism

The VPH grating inheres ideal diffraction efficiency on a higher dispersion spectroscopy at a specific wavelength region, otherwise, diffraction efficiencies decrease on higher order diffractions. We propose an grism consists a comb like grating (Fig. 8), we called quasi-Bragg grating, and two high-index prisms. The quasi-Bragg grism has both advantage of VPH and Echell type grism (Fig. 9) [17-18]. We are developing a comb like grating by means of semiconductor process.

3. Immersion Grating

3.1. Mid-infrared high dispersion spectrograph

IRHS is under planning design study as a next generation instrument for the 8.2m Subaru telescope. IRHS is aiming resolving power of $R = \lambda/\Delta\lambda = 200,000$ at $10\mu\text{m}$, in order to observe vibrational transitions of molecule in circum-stellar and dark clouds for instance. Such a high dispersion spectrograph requires a dispersing element or moving mirror with minimum 2m in an optical path difference. A Fourier transform spectrometer (FTS) is usually applied as a high dispersion spectrometer for laboratory use from middle to far infrared because of the small size and low cost of the instrument compared with a grating spectrometer. Although FTS has disadvantages with background noise and atmospheric turbulence, only several tens or hundreds astronomical objects in the total sky can be observed around $10\mu\text{m}$. On the other hand, a mid-infrared high dispersion spectrograph with a conventional grating of reflection type (Fig.1a) as the dispersing element requires a large optical installation. Since a collimated beam of 40cm in diameter should be used for the conventional grating spectrograph with a resolving power of 200,000 at $10\mu\text{m}$, the total volume of the instrument covered with a cooled vacuum chamber (below 50K) is nearly 100m^3 . It is huge enough even for the Nathmith focus of the Subaru telescope.

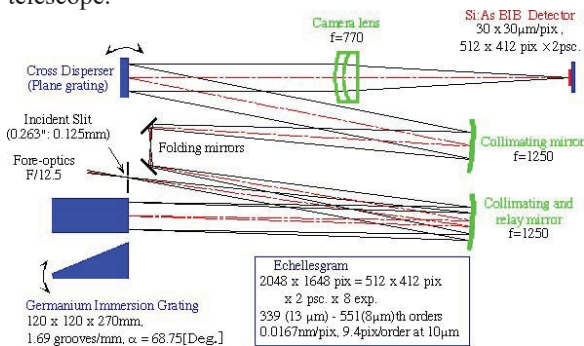


Fig. 10 Mid-infrared high dispersion spectrograph with $R=100,000@10\mu\text{m}$ for SPICA (3.5m space infrared observatory)

3.2. Trial fabrications for solid gratings

The germanium immersion grating for instance could reduce 1/64 as the total volume of a spectrograph with a conventional reflection grating since refractive index of germanium is over 4.0 from 1.6 to $20\mu\text{m}$. The size of IRHS become 2m^3 covered with a cooled vacuum chamber [19]. The immersion grating is not only a powerful dispersion element for grand-based applications, but also an ideal dispersion element for space applications (Fig.10).

In order to fabricate a solid grating with a high index material, numerous studies on micro-machining methods have been carried out by researchers and engineers. These include a precise ruling-engine, anisotropic chemical etching and so on [20-24]. To our knowledge, the KRS-5 grism used for near to middle infrared can be fabricated by using a precise ruling-engine [23]. However, since KRS-5 is a mixed crystal of TlBr and TlI, a homogeneous and large block is difficult to grow.

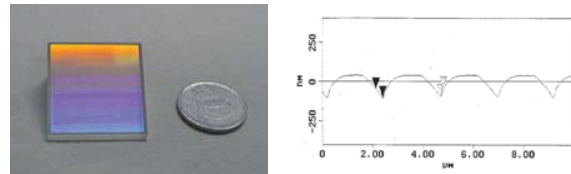


Fig. 11 Lithium niobate grism fabricated by oblique ion etching (left) and cross section of the grism (right).

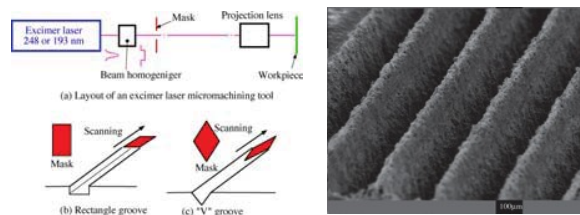


Fig. 12 Schematic representation of grating fabrication by laser abrasion (left) and SEM picture of germanium grooves fabricated by laser abrasion (right).

We had also performed trials of various methods for grating fabrications, resinous bonded diamond grinding, ion etching (Fig. 11) and laser ablation (Fig. 12) [25-27], for example. However solid gratings with deep grooves exceed $1\mu\text{m}$ in depth, are difficult to fabricate with these methods. Finally, we had successfully fabricated an immersion grating for the prototype IRHS by using a 3D profile grinding/turning machine with nano precision and grinding cups of cast iron with electrolytic dressing method (Fig. 13, 14) [28-31].

3.3. Fabrication of immersion grating

The immersion gratings of prototype IRHS were designed for a spectrograph with a resolving power of 50,000 at $10\mu\text{m}$ or 250,000 at $2.0\mu\text{m}$. The sizes of the prototype immersion gratings are 30 x 30 mm, 72mm in length and vertex angle of 68.75 degree. Groove

spacing are $100\mu\text{m}$ for the first, $250\mu\text{m}$ for the second and third, $600\mu\text{m}$ for the fourth and fifth fabrications. The grooves are slightly tilted to the incident aperture of the gratings to avoid influence of reflection at the incident aperture. The material of the immersion grating was germanium single crystal except the third fabrication. At the third fabrication, GaAs single crystal was chosen for the immersion grating because it was planned to use for a near infrared spectrograph, and GaAs is transparent from $0.9\mu\text{m}$ and its refractive index is about 3.4 at $1.0\mu\text{m}$.

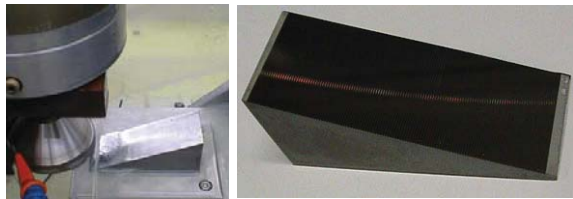


Fig. 13 Fabrication of germanium immersion grating by means of nano-precision machine (left) and picture of prototype immersion grating for IRHS (right).

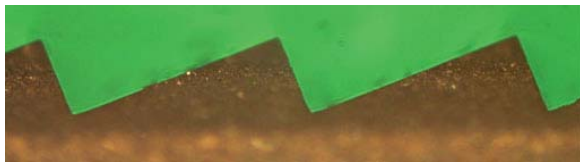


Fig. 14 Grooves shape of immersion grating fabricated by grinding cups of cast iron and electrolytic dressing method.

The wave front error of the fourth and fifth grating are acceptable for a prototype immersion grating at $10\mu\text{m}$ if the maximum value of wave front error inside germanium is set up one eighth wave in rms, that is, 312.5nm in the air. We had obtained doubtful values of transmittance measured by using a conventional spectrophotometer because grooves are tilted about 0.8 degree to the incident aperture, and an incident and exit ray are angled about 3.2 degrees at a groove. We could say that the diffraction efficiency of the third, fourth and fifth gratings are at least 30% from 2 to $16\mu\text{m}$. Accurate diffraction efficiencies of gratings will measure by the prototype IRHS of under construction.



Fig. 15 Measurement of far-field image of immersion grating.

Figure 15 shows measurement for far field images of a diffraction beam. A beam of the CO_2 laser as a light source at $10.6\mu\text{m}$ was transformed to a Gaussian beam by means of a spatial filter. Figure 16 shows the cross sections of the far field images of an incident aperture and the diffraction beams of the gratings mentioned above. The dotted line is a far field image of the reflected beam of the incident aperture. The solid lines are the far field images of diffracted beams of immersed grooves. The FWHM of the ideal image for the measurement system is $220\mu\text{m}$. The FWHM of the images of the third, fourth and fifth gratings are 280 , 259 and $302\mu\text{m}$ respectively. The far field image of the third grating has side lobes with large amplitude caused by fatal wave front error. The FWHM of far field images of the fourth grating expands 18% which is compared with the ideal image, and it is seen a Roland ghost which amplitude is about 17% of the main lobe. The FWHM of the fifth grating expands 37%, and it is seen a Roland ghost which amplitude is about 14% of the main lobe. The expansion and Roland ghost implies a wave front error with large scale of a grating, that is, a deviation of the groove interval.

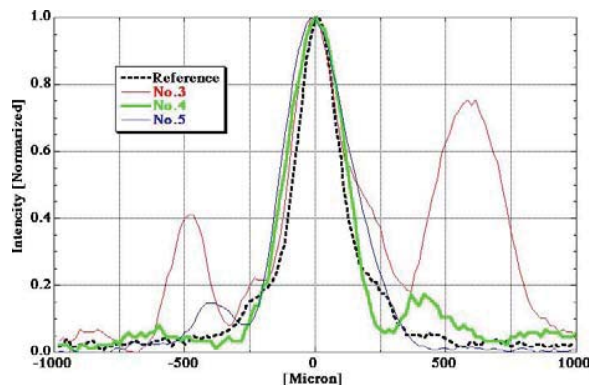


Fig. 16 Cross section of far-field image of immersion gratings. No. 4: $R=44,000@10\mu\text{m}$.

4. Conclusion

The SR grism is suitable for low dispersion spectroscopy with wide wavelength range, while the VPH grism is an ideal dispersing element for high dispersion spectroscopy with a specific wavelength region. Furthermore the “Quasi-Bragg grism” will open up high dispersion spectroscopy with wide wavelength range.

Although further improvement for the wave front profile should be done, the results of the trial fabrication suggest that a germanium immersion grating used at around $10\mu\text{m}$ can be realized by means of a 3D profile grinding/turning machine with nano precision and grinding cups of cast iron with electrolytic dressing method.

5. APENDIX A

As shown in figure 4, Snell's equation of refraction for the incident surface and boundary between prism and VPH grating of the VPH grism are given by

$$\sin \alpha = n_1 \sin \theta_1 \quad (1)$$

$$n_1 \sin(\alpha - \theta_1) = n_2 \sin \theta_2 \quad (2)$$

In the case of critical angle, θ_2 is right angle, that is, $\sin \theta_2$ is 1.0 and then Eq.2 is rewritten as:

$$\sin(\alpha - \theta_1) = \frac{n_2}{n_1} \quad (3)$$

From Eq.3, Eq.1 is rewritten as:

$$\begin{aligned} \sin \alpha &= n_1 \sin \left\{ \alpha - \sin^{-1} \left(\frac{n_2}{n_1} \right) \right\} \\ &= n_1 \sin \alpha \cos \left\{ \sin^{-1} \left(\frac{n_2}{n_1} \right) \right\} \\ &\quad - n_1 \cos \alpha \sin \left\{ \sin^{-1} \left(\frac{n_2}{n_1} \right) \right\} \\ \tan \alpha &= \frac{n_2}{n_1 \cos \left\{ \sin^{-1} \left(\frac{n_2}{n_1} \right) \right\} - 1} \\ &= \frac{n_2}{n_1 \cos \left\{ \cos^{-1} \left(\frac{\sqrt{n_2^2 - n_1^2}}{n_1} \right) \right\} - 1} \\ &= \frac{n_2 \left(\sqrt{n_2^2 - n_1^2} + 1 \right)}{n_2^2 - n_1^2 - 1} \quad (4) \end{aligned}$$

6. REFERENCES

1. N. Ebizuka, K. Oka, A. Yamada, M. Ishikawa, M. Kashiwagi, K. Kodate, Y. Hirahara, S. Sato, W. Fuji, M. Wakaki, K.S. Kawabata, M. Watanabe, H. Suto, M. Tamura and M. Iye, "Grism and Immersion Grating for the 8.2m Subaru Telescope", *Diffractive Optics 2003*, 118-119, 2003.
2. N. Ebizuka, H. Kobayashi, Y. Hirahara, M. Wakaki, K. Kawaguchi, T. Sasaki and M. Iye "Development of grisms and immersion gratings for the spectrographs of the Subaru Telescope" *Imaging the Universe in Three Dimensions*, eds. W. van Breugel and J. Bland-Hawthorn, *A.S.P. Conf. Ser.*, **195**, 564-567, 1999.
3. N. Ebizuka, M. Iye, T. Sasaki and M. Wakaki, "Development of High dispersion grisms and immersion gratings for spectrographs of Subaru Telescope", *Proc. SPIE*, **3355**, 409-416, 1998
4. Design and Applications Handbook Photonics 1995 pp.H-372
5. K. Oka, W. Klaus, M. Fujino, M. Watanabe, N. Ebizuka and K. Kodate, "Rigorous Analysis of a Volume Phase Holographic Grism for Astronomical Observations", *Congress of International Communication for optics (ICO)*, **19**, 565-566, 2002.
6. S.C. Barden, J.A. Arns, W.S. Colburn and J.B. Williams, "Volume-Phase Holographic Gratings and the Efficiency of Three Simple Volume-Phase Holographic Gratings", *Publ. Astron. Soc. Pacific*, **112**, 809-820, 2001
7. M. Kawabata, A. Sato, I. Sumiyoshi and T. Kubota, "Photopolymer system and its application to color hologram", *Appl. Opt.* **33**, 2152-2156, 1994.
8. K. Oka, A. Yamada, Y. Komai, E. Watanabe, N. Ebizuka, T. Teranishi, M. Kawabata and K. Kodate, "Optimization of a Volume Phase Holographic Grism for Astronomical Observation using the Photopolymer", *Proc. SPIE*, **5005**, 8-19, 2003.
9. N. Kaifu, "Subaru telescope", *Proc. SPIE*, **3352**, 14-22, 1998.
10. N. Kaifu et al., "The First Light of the Subaru Telescope: A New Infrared Image of the Orion Nebula", *Publ. Astron. Soc. Jpn.*, **52**, 1-8 and Plate 1-5, 2000.
11. M. Iye et al., "Subaru first-light deep photometry of galaxies in A851 field", *Publ. Astron. Soc. Jpn.*, **52**, 9-24, 2000.
12. N. Kashikawa, M. Inata, M. Iye, K. Kawabata, K. Okita, G. Kosugi, Y. Ohyama, T. Sasaki, K. Sekiguchi, T. Takata, Y. Shimizu, M. Yoshida, K. Aoki, Y. Saito, R. Asai, H. Taguchi, N. Ebizuka, T. Ozawa, Y. Yadoumaru, "FOCAS: Faint Object Camera and Spectrograph for the Subaru Telescope", *Proc. SPIE*, **4008**, 104-113, 2000.
13. Y. Ohyama, M. Yoshida, T. Takata, M. Imanishi, T. Usuda, Y. Saito, H. Taguchi, N. Ebizuka, F. Iwamuro, K. Motohara, T. Taguchi, T. Hata, T. Maihara, M. Iye, T. Sasaki, G. Kosugi, R. Ogasawara, J. Noumaru, Y. Mizumoto, M. Yagi and Y. Chikada, "Superwind-Driven Intense H₂ Emission in NGC 6240", *Publ. Astron. Soc. Jpn.*, **52**, 563-576 and Plate 43-44, 2000.
14. K.S. Kawabata, N. Ebizuka, T. Sasaki, K. Sekiguchi, M. Iye, K. Aoki, R. Asai, M. Inata, N. Kashikawa, G. Kosugi, T. Misawa, Y. Ohyama, K. Okita, T. Ozawa, Y. Saito, Y. Shimizu, H. Taguchi, T. Takata, Y. Yadoumaru, M. Yoshida, "Properties of FOCAS optical components", *Proc. SPIE*, **4841**, 1219-1228, 2003.
15. N. Ebizuka, K. Oka, A. Yamada, M. Watanabe, K. Shimizu, K. Kodate, M. Kawabata, T. Teranishi, K.S. Kawabata, M. Iye, "Development of Volume Phase Holographic (VPH) Grism for Visible to Near Infrared Instruments of the

- 8.2m Subaru Telescope", *Proc. SPIE*, **4842**, 319-328, 2003.
16. A. Yamada, K. Oka, M. Ishikawa, M. Kashiwagi, K. Kodate, N. Ebizuka and T. Teranishi, "Spectroscopic Observation for the Subaru Telescope", *Diffraction Optics 2003*, 110-111, 2003.
17. K. Oka, N. Ebizuka and K. Kodate, "Rigorous Analysis of a Quasi-Bragg Diffraction Grating for Astronomical Observation", *Diffraction Optics 2003*, 46-47, 2003.
18. K. Oka, N. Ebizuka and K. Kodate, "Optimal design of the grating with reflective plate of comb type for astronomical observation using RCWA", *Proc. SPIE*, **5290**, in press, 2004.
19. H. Tokoro, M. Atarashi, M. Omori, T. Machida, S. Hirabayashi, H. Kobayashi, Y. Hirahara, T. Masuda, N. Ebizuka and K. Kawaguchi, "Development of a mid-infrared high dispersion spectrograph (IRHS) for the Subaru telescope", *Proc. SPIE*, **4841**, 1016-1025, 2003.
20. H. Dekker, "An Immersion Grating for an Astronomical Spectrograph", *Instrumentation for Ground-Based Optical Astronomy, Present and Future*, ed, L.B. Robinson, *IGBO.conf.* **183**, 183-188, 1988.
21. G. Wiedemann and D.E. Jennings, "Immersion grating for infrared astronomy", *Appl. Opt.*, **32**, 1176-1178, 1993.
22. H.U. Kaufl and B. Delabre, "Improved Design and Prototyping for a 10/20 mm Camera/Spectro-meter for ESO's VLT", *Proc. SPIE*, **2198**, 1036-1046, 1994.
23. M. Shure, D.W. Toomey, J.T. Rayner, P.M. Onaka and A.T. Denault, "NSFCAM: a new infra-red array camera for the NASA Infrared Telescope Facility", *Proc. SPIE*, **2198**, 614-622, 1994.
24. L. Weitzel, A. Krabbe, H. Kroker, N. Thatte, L.E. Tacconi-Garman, M. Cameron and R. Genzel, "3D: The next generation near-infrared imaging spectrometer", *Astron. Astrophys. Suppl. Ser.* **119**, 531-546, 1996.
25. N. Ebizuka, M. Iye and T. Sasaki, "Optically Anisotropic Crystalline Grisms for Astronomical Spectrographs", *Appl. Opt.* **37**, 1236-1242, 1998.
26. Y. Aoyagi and S. Nanba, "Blazed ion-etched holographic gratings" *Optica Acta* **23**, 701-707, 1976.
27. P.T. Rumsby, E.C. Harvey and D.W. Thomas, "Laser Microprojection for Micromechanical Device Fabrication", *Proc. SPIE*, **2921**, 684-692, 1996.
28. N. Ebizuka, S. Morita, T. Shimizu, Y. Yamagata, H. Omori, M. Wakaki, H. Kobayashi, H. Tokoro, Y. Hirahara, "Development of Immersion Grating for Mid-Infrared High Dispersion Spectrograph for the 8.2m Subaru Telescope", *Proc. SPIE*, **4842**, 293-300, 2003.
29. H. Ohmori, N. Ebizuka, S. Morita, Y. Yamagata, "Ultraprecision micro-grinding of germanium immersion grating element for mid-infrared super dispersion spectrograph", *CIRP 51st General Assembly*, 221-224, 2001.
30. N. Ebizuka, S. Morita, Y. Yamagata, H. Ohmori, K. Kawaguchi, M. Wakaki, H. Kobayashi, Y. Hirahara, "Mid-infrared high dispersion spectrograph (IHR) for the Subaru telescope: development of immersion gratings", *Diffraction Optics 2001*, 12-13, 2001.
31. N. Ebizuka, S. Morita, H. Ohmori, Y. Yamagata, H. Kobayashi, Y. Hirahara, M. Wakaki and K. Kawaguchi "Development of immersion gratings for Subaru Telescope by means of ELID grinding method", *Advances in Abrasive Technology*, **III**, eds. N. Yasunaga, J. Tamaki, K. Suzuki and T. Uematsu, *The Soc. of Grinding Engineers Jpn*, **149-154**, 2000, ISBN 4-99000662-1-9.